MPC-based time synchronization method for V2V (vehicle-to-vehicle) communication

Yong Chen and Zhixian Zhan
School of Electronic and Information Engineering, Lanzhou Jiaotong University, Lanzhou, China, and
Wei Zhang
School of Traffic and Transportation, Lanzhou Jiaotong University, Lanzhou, China

Received 20 January 2023
Revised 6 February 2023
Accepted 6 February 2023

Abstract

Purpose – As the strategy of 5G new infrastructure is deployed and advanced, 5G-R becomes the primary technical system for future mobile communication of China's railway. V2V communication is also an important application scenario of 5G communication systems on high-speed railways, so time synchronization between vehicles is critical for train control systems to be real-time and safe. How to improve the time synchronization performance in V2V communication is crucial to ensure the operational safety and efficiency of high-speed railways.

Design/methodology/approach – This paper proposed a time synchronization method based on model predictive control (MPC) for V2V communication. Firstly, a synchronous clock for V2V communication was modeled based on the fifth generation mobile communication-railway (5G-R) system. Secondly, an observation equation was introduced according to the phase and frequency offsets between synchronous clocks of two adjacent vehicles to construct an MPC-based space model of clock states of the adjacent vehicles. Finally, the optimal clock offset was solved through multistep prediction, rolling optimization and other control methods, and time synchronization in different V2V communication scenarios based on the 5G-R system was realized through negative feedback correction.

Findings – The results of simulation tests conducted with and without a repeater, respectively, show that the proposed method can realize time synchronization of V2V communication in both scenarios. Compared with other methods, the proposed method has faster convergence speed and higher synchronization precision regardless of whether there is a repeater or not.

Originality/value – This paper proposed an MPC-based time synchronization method for V2V communication under 5G-R. Through the construction of MPC controllers for clocks of adjacent vehicles, time synchronization was realized for V2V communication under 5G-R by using control means such as multistep prediction, rolling optimization, and feedback correction. In view of the problems of low synchronization precision and slow convergence speed caused by packet loss with existing synchronization methods, the observer equation was introduced to estimate the clock state of the adjacent vehicles in case of packet loss, which reduces the impact of clock error caused by packet loss in the synchronization process and improves the synchronization precision of V2V communication. The research results provide some theoretical references for V2V synchronous wireless communication under 5G-R technology.

Keywords V2V communication, 5G-R, Time synchronization, MPC, High-speed railway

Paper type Research paper

This research was supported by the National Natural Science Foundation of China (Grant Nos. 61963023 & 61841303) and the Tianyou Innovation Team Science Foundation of Lanzhou Jiaotong University (Grant No. TY202003).

Railway Sciences
Vol. 2 No. 1, 2023
pp. 101-120
Emerald Publishing Limited
e-ISSN: 2755-0915
p-ISSN: 2755-0907
DOI 10.1108/RS-01-2023-0002

1. Introduction

The train control system, central to high-speed railways, consists of core technical equipment that ensures the operational safety and improves the operational efficiency of high-speed railways. At present, Chinese Train Control System Level 3 (CTCS-3) uses a train-ground communication system for the bidirectional transmission of train control information (Dou, Li, Li, Bao, & Lin, 2021). However, the rapid development of high-speed railways raises higher requirements for operational efficiency and safety protection.

As the strategy of 5G "new infrastructure" is deployed and advanced, 5G-R (the fifth generation mobile communication-railway) becomes the primary technical system for future mobile communication of China's railway. It can provide a wide-bandwidth and high-reliability wireless access guarantee for the train control system (Wang, 2020). As an important application scenario of 5G-R, communication between trains (V2V communication) can further improve the operational safety and efficiency of train control services. However, in the process of V2V communication under 5G-R, the V2V communication link is characteristic of time variation (Ding, 2020) due to the high-speed mobility of trains, resulting in the degradation of synchronization performance. How to improve the time synchronization performance in V2V communication is crucial to ensure the operational safety and efficiency of high-speed railways.

Based on different V2V communication scenarios with and without a repeater (Wang, Li, & Li, 2016), the current methods used to realize time synchronization can be divided into centralized time synchronization methods and distributed time synchronization methods (Koo & Mahyuddin, 2019). The centralized methods generally need a reference node to provide a reference time for the synchronization process. Shi, Tuo, Yang, Lu, and Li (2020) proposed a fast-flooding, multi-channel, unidirectional broadcast time synchronization protocol, which realizes time synchronization by flooding the reference time along a multi-hop path to a whole network, but once packet loss occurs at the single node, the synchronization precision of the whole network will be affected. Wang, Qi, and Li (2020) introduced proportional integral derivative (PID) control in the time synchronization process to reduce the interference error, but it could not adapt to the clock jump caused by fast time variation. Son and Chang (2020) proposed a clock synchronization method based on the precision time protocol (PTP) to estimate the information of the faulty node by collecting and analyzing the clock information of other nodes, but this method does not take into consideration the factor of packet loss, thus leading to inaccurate estimates. Shivaaraman, Schuster, Ramanathan, Easwaran, and Steinhorst (2021) proposed a cluster-based time synchronization protocol, but this method cannot reduce the synchronization error caused by packet loss. Jia, Wang, and Zheng (2020) proposed a clock synchronization protocol based on clustering algorithms, but this method did not take into consideration the impact of packet loss on the synchronization process.

For distributed time synchronization methods, the average time synchronization (ATS) theory is generally used to realize time synchronization between both communication sides (Schennato & Fiorentin, 2011) because there is no repeater to transmit reference time. Wang, Chen, Gong, and Li (2020) used the ATS time synchronization method to compensate for the clock offset estimate obtained by using the weighted median. Shi, Tuo, Ran, Ren, and Yang (2020) proposed a multi-hop average consensus time synchronization method to enhance algebraic connectivity of the network and improve convergence speed through virtual links. Phan and Kim (2021) proposed a virtual topology time synchronization method based on ATS to speed up convergence. However, compared with centralized synchronization methods, the distributed time synchronization methods mentioned above generally have the disadvantage of slow convergence speed (Koo & Mahyuddin, 2019) and cannot adapt to the fast time variation of 5G-R wireless channels. To sum up, the current methods proposed in most studies for time synchronization in V2V communication do not consider the impact of

packet loss on synchronization, thus leading to problems such as low synchronization precision and algorithm convergence speed.

In this paper, a time synchronization method based on model predictive control (MPC) was proposed for V2V communication under 5G-R. A synchronous clock model was established for V2V communication under 5G-R, and an observation equation was introduced to build the MPC-based space model and incremental prediction model of clock states of adjacent vehicles. Time synchronization was realized for V2V communication in different scenarios through control modes including multistep prediction, rolling optimization and negative feedback regulation.

2. Analysis of time synchronization in V2V communication under 5G-R

The proximity service technology in the 5G standard supports V2V communication technology (Lai, Shieh, Chou, & Hsu, 2020). V2V communication technology is divided into two scenarios: direct communication without a repeater and indirect communication through repeater stations. In the latter scenario, information exchange between adjacent trains is indirectly completed through the Next Generation NodeB (gNB), as shown in Figure 1.

High-precision time synchronization between adjacent trains is the key to V2V communication. Time synchronization in V2V communication under 5G-R requires time precision to be better than ± 50 ms (Teng, 2021). The higher the time synchronization precision, the more key real-time control information such as speed and location of adjacent trains, and the more conducive to improving the operation safety of trains. In order to reach the required high precision of the V2V communication link, time synchronization between

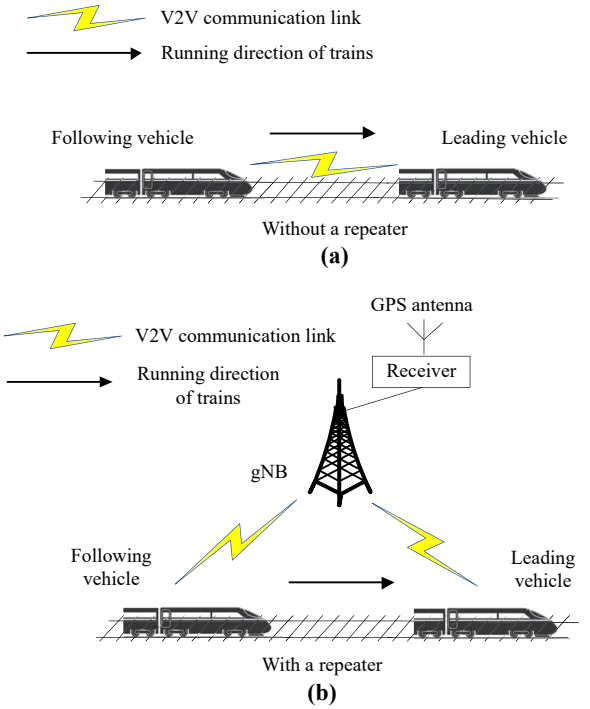

Figure 1.
Schematic diagram of 5G-R V2V communication scenario

adjacent vehicles needs to be measured by the PTP protocol. The PTP protocol can reach synchronization precision of sub-microsecond level, and can provide high-precision time service for equipment to support high-precision time synchronization and synchronous measurement requirements of V2V communication and other services (Seijo, López-fernández, Bernhard, & Val, 2020; Teng, 2021). As a time synchronization protocol for a bidirectional information exchange mechanism, the master and slave clocks complete time synchronization by exchanging PTP messages carrying timestamps (Figure 2). Wherein, i is the clock nodes of adjacent vehicles, in $i \in \{1, 2\}$; T_1, T_2, T_3, and T_4 are the timestamps when PTP messages are transmitted between the reference clock and the vehicle clocks, respectively; θ is the time offset between the reference clock and the vehicle clocks; d is the path delay between the reference clock and the vehicle clocks.

It is generally assumed that the transmission path of PTP messages is symmetrical between the master and slave clocks, and then the clock offset θ_i between the adjacent vehicles and the reference clock is

$$\theta_i = \frac{(T_{2,i} - T_1) - (T_4 - T_{3,i})}{2} \tag{1}$$

The path delay d_i between the adjacent vehicles and the reference clock is

$$d_i = \frac{(T_{2,i} - T_1) + (T_4 - T_{3,i})}{2} \tag{2}$$

The time deviation between the adjacent vehicles and the reference clock can be calculated from Equations (1) and (2), thus realizing time synchronization with the reference clock.

In the process of V2V communication under 5G-R, whether there is a repeater or not, the goal of time synchronization between adjacent vehicles is achieved by dynamically adjusting the local clock $S_i(t)$ of the adjacent vehicles against and finally aligning it to the standard reference clock $L(t)$. The time synchronization process in V2V communication refers to the setting of time $S(t)$ and needs to be adjusted according to different V2V communication scenarios.

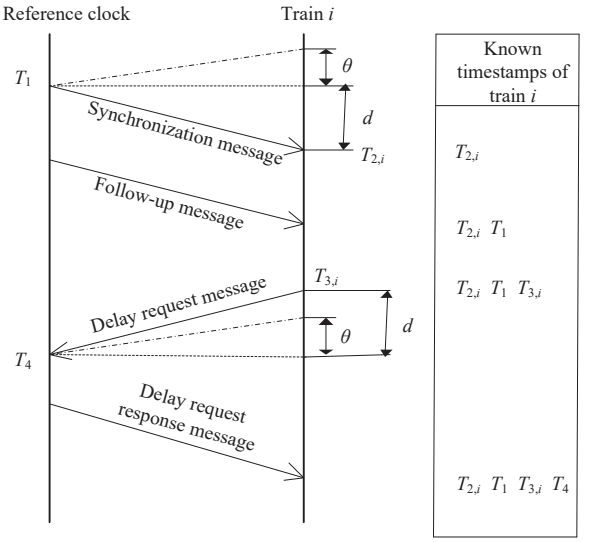

Figure 2.
Time synchronization process in V2V communication under 5G-R

(1) When there is a repeater in V2V communication, the repeater station gNB obtains the standard time signal through the built-in GPS receiver, and thus gNB can be set as the reference clock. In this scenario, if the maximum error $e(t)$ between the local time $S_i(t)$ of the adjacent vehicles and the reference time satisfies Equation (3) below:

$$\lim_{t\to\infty} e(t) = \max(S(t) - S_i(t)) = 0 \tag{3}$$

The time synchronization process is completed for V2V communication with a repeater.

(2) When V2V communication is in a scenario without a repeater, a virtual reference clock needs to be set since there is no physical reference clock to provide standard time. At this time, adjacent vehicles can be regarded as independent intelligent agents, and the time of the virtual reference clock can be dynamically set through the exchange of time information. The local time $S_i(t)$ of the adjacent vehicles is kept consistent with the virtual reference time, thus realizing the time synchronization between the vehicles, that is

$$S_i(t) = c(t) \tag{4}$$

where $c(t)$ is the virtual reference time.

3. Establishment of synchronous clock models for V2V communication

3.1 Ideal clock model

In the process of time synchronization in V2V communication, a synchronization clock model was established first, and the adjacent vehicles and the repeater station gNB were equipped with local clock modules. Thanks to the built-in high-precision voltage-controlled crystal oscillator, the local time of the clock module of the repeater station gNB can remain stable (Fan, Liu, Li, & Chen, 2021). And with ordinary crystal oscillators built in, clock modules of the adjacent vehicles are susceptible to external environmental factors such as temperature and pressure on account of their physical characteristics, and the crystal oscillators will suffer from random jitter of varying extent, resulting in clock frequency and phase offsets. The phase offset $\theta_i(t)$ between different clocks of the adjacent vehicles and the reference clock can be defined as

$$\theta_i(t) = \theta_{0i} + \int_0^t \alpha_i(\tau)\mathrm{d}\tau + \varphi_{i\theta}(t) \tag{5}$$

where θ_{0i} is the initial clock phase offset of node i; $\alpha_i(\tau)$ is the clock frequency offset of node i at time τ; $\varphi_{i\theta}(t)$ is the random clock phase jitter caused by environmental changes of node i at time t.

Similarly, the clock frequency offset $\alpha_i(t)$ between different clocks of the adjacent vehicles and the reference clock t can be defined as

$$\alpha_i(t) = \alpha_{0i} + \varphi_{i\alpha}(t) \tag{6}$$

where α_{0i} is the initial clock frequency offset of node i; $\varphi_{i\alpha}(t)$ is the random clock frequency jitter of node i at time t.

To solve clock synchronization in MPC-based V2V communication, it is necessary to discretize the continuous differential Equations (5) and (6) since the MPC solution is based on the discrete space state equation of the controlled object. The following equations were obtained

$$\theta_i(k) = \theta_i(k-1) + \alpha_i(k-1)\tau(k) + \omega_{i\theta}(k) \tag{7}$$

$$\alpha_i(k) = \alpha_i(k-1) + \omega_{i\alpha}(k) \tag{8}$$

where k is the number of time synchronization cycles, $k = 1, 2, \ldots$; $\omega_{i\theta}(k)$ is the clock phase jitter of the k-th time synchronization cycle and is normally distributed with zero mean and variance of σ_θ^2; $\omega_{i\alpha}(k)$ is the frequency jitter of the k-th time synchronization cycle and is normally distributed with zero mean and variance of σ_α^2.

3.2 Actual clock model

After the ideal clock model for V2V communication is established, an actual clock model for V2V communication needs to be additionally established.

In the process of actual time synchronization in V2V communication under 5G-R, PTP messages, affected by the fast time variation of 5G-R wireless channels, will suffer from link asymmetry, random jitter of transmission delay, and packet loss, when transmitted on the V2V communication link (Novaes, Freire, Klautau, & Almeida, 2021). The above problems will cause uncertainty errors in PTP timestamps, which will seriously affect the time precision of PTP protocol on the V2V communication link. In general, the uncertainty timestamp error is assumed to be random noise following a Gaussian distribution, so the phase offset $\theta_{i\mathrm{M}}$ in the actual clock model of the adjacent vehicles is

$$\theta_{i\mathrm{M}}(t) = \frac{(T_{2,i} - T_{1,i}) - (T_4 - T_{3,i})}{2} + v_{i\theta}(t) \tag{9}$$

where $v_{i\theta}$ is the random noise of clock phase offset, and its values are normally distributed with a mean of 0 and a variance of $\sigma_{i\mathrm{M}}^2$.

4. Time synchronization methods for V2V communication under 5G-R

Demonstrating clock synchronization in V2V communication with a model, this paper proposed an MPC-based time synchronization method for V2V communication under 5G-R to improve the performance and efficiency of V2V communication synchronization. MPC is a model-based closed-loop optimal control method and has the characteristics of fast transient response and high control bandwidth, making it suitable for fast time-varying scenarios (Alfaro, Guzman, De Vicuña, Miret, & Castilla, 2022).

With the method in this paper, the reference clock for time synchronization tracking of the adjacent vehicles was set for different scenarios of V2V communication. Then, the clock states of adjacent vehicles are used as inputs to the MPC controllers of adjacent vehicles, respectively. Through the predicted output of MPC input, iterative rolling optimization and feedback correction, consistency tracking between the adjacent vehicles and the reference clock was realized, and time between vehicles was synchronized. Figure 3 shows how the MPC controllers in this paper were established. In the figure, $r(k)$ is the reference clock selected for MPC controllers according to different V2V communication scenarios, either being the clock of the repeater station gNB, or if there is no repeater, being dynamically set through the exchange of time information between the adjacent vehicles; $u_i(k)$ is the control input; $y_i(k)$ is the clock state output of the adjacent vehicles; $\bar{y}_i(k)$ is the predicted output of the current train clock state; $\bar{y}_i(k+n|k)$ is the train clock state output for the next n synchronization cycles.

After the reference clock was selected for the communication scenario, time was synchronized between vehicles through the MPC controllers established for the adjacent vehicles. The specific steps are as follows.

Step 1: Based on synchronous clock models for V2V communication, establish a clock state space model with MPC for V2V communication and obtain the corresponding clock state output $y_i(k)$ of the adjacent vehicles.

Step 2: Build a predictive model according to the clock state of the current train to obtain the predicted output $\bar{y}_i(k)$ of the current train clock state.

Step 3: According to the current predicted output $\bar{y}_i(k)$ and the control input $\boldsymbol{u}_i(k)$, the train clock state in the next n synchronization cycles is predicted to obtain the predicted output $\bar{y}_i(k+n|k)$.

Step 4: Design a cost function J in the form of a quadratic matrix to minimize the deviation between the predicted output $\bar{y}$ and the actual output y, and take a rolling-horizon quadratic-programming approach to obtain the optimal solutions of different input control $\boldsymbol{u}_i$ of the adjacent vehicles in the next synchronization cycle. Finally, perform feedback correction with the optimal control input $\boldsymbol{u}_i$ and iterate the above steps for the adjacent vehicles to track the reference clock through the correction with $\boldsymbol{u}_i$, thus synchronizing the time between vehicles.

4.1 State space model

According to the MPC-based synchronization steps for V2V communication, a state space model for V2V communication needs to be established first. As an optimal control method based on the state space model (Zhang, Wu, Teng, Gong, & Tang, 2022), MPC predicts the state and output of the adjacent vehicle clocks at future moments through the state space model. Figure 4 shows the specific process of the state space model.

As can be seen, the state space model for synchronization in V2V communication in this paper consists of a general state equation and an observation equation. In a certain synchronization cycle k, if no PTP message is lost, that is, the clock states of the adjacent vehicles can be accurately measured through PTP message transmission, the accurate clock

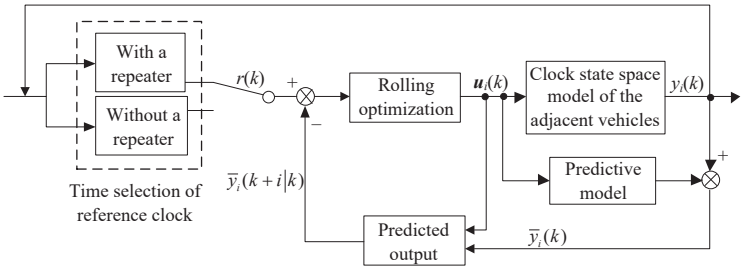

Figure 3.
Schematic diagram of establishing MPC of the adjacent vehicles

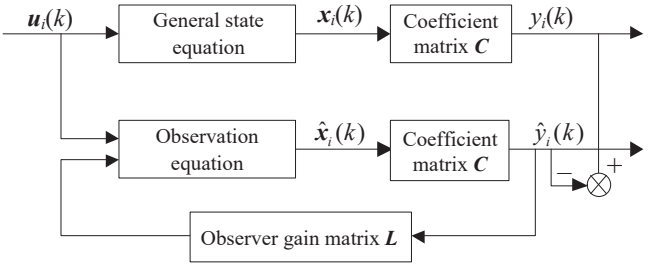

Figure 4.
Schematic diagram of establishing clock state space model

states $\boldsymbol{x}_i(k)$ of the adjacent vehicles in the k-th cycle can be calculated from the general state equation, and then the standard reference clock $y_i(k)$ for clock state output can be obtained through the dimensional coefficient matrix $\boldsymbol{C}$. If PTP message loss occurs, meaning that the clock states of the adjacent vehicles cannot be accurately measured, it is necessary to introduce the observation equation, observe the output estimate $\widehat{y}_i(k)$ obtained from the observation equation through the gain matrix $\boldsymbol{L}$ and perform negative feedback adjustment, so that the output estimate value $\widehat{y}_i(k)$ of the clock states of the adjacent vehicles obtained by the observer can be infinitely close to the standard reference $y_i(k)$ and the V2V synchronization process can be completed.

For the establishment of the observation equation in Figure 4, in the scenario with a repeater, Equations (7)–(9) can be combined, and the control input $\boldsymbol{u}$ can be added so that the adjacent vehicles are consistent with the gNB reference time by continuously adjusting $\boldsymbol{u}$. Since there is no accurate physical reference clock in the repeater-free scenario, the virtual reference clock time $c(t)$ in Equation (4) needs to be dynamically adjusted according to the time of the adjacent vehicles so as to realize V2V synchronization. Therefore, according to the characteristics of the two V2V communication scenarios, the MPC state-space model of the time synchronization process of V2V communication under different scenarios was established as

$$\begin{aligned}\boldsymbol{x}_i(k+1) &= \boldsymbol{A}\boldsymbol{x}_i(k) + \boldsymbol{B}\boldsymbol{u}_i(k) + \boldsymbol{\omega}_i(k) = \\ &(1-\beta)\boldsymbol{x}_i(k) + \beta\boldsymbol{x}_j(k)\end{aligned} \tag{10}$$

$$y_i(k) = \boldsymbol{C}\boldsymbol{x}_i(k) + \nu_i(k) \tag{11}$$

with

$$\boldsymbol{A} = \begin{pmatrix} 1 & \tau \\ 0 & 1 \end{pmatrix}$$

$$\boldsymbol{B} = \begin{pmatrix} 1 \\ 1 \end{pmatrix}$$

$$\boldsymbol{\omega}_i(k) = \begin{pmatrix} \omega_{i\theta}(k) \\ \omega_{i\alpha}(k) \end{pmatrix}$$

$$\boldsymbol{C} = \begin{pmatrix} 1 & 0 \end{pmatrix}$$

where $\boldsymbol{x}_i$, $\boldsymbol{u}_i$ and y_i are the state, the control input and the output of train clock node i, respectively; $\boldsymbol{A}$, $\boldsymbol{B}$ and $\boldsymbol{C}$ are matrixes of appropriate dimensions, determined by the system; $\boldsymbol{\omega}_i$ and ν_i are the system input disturbance and the output disturbance caused by the uncertainty of 5G-R wireless channel, respectively; β is the dynamic coefficient; $\boldsymbol{x}_j(k)$ is the clock state of train clock node j at the current time.

In the actual V2V communication process, losing clock information transmitted via PTP is inevitable due to the complex and changing environment of the 5G-R wireless channel. This makes it impossible for clock state measurements of the adjacent vehicles to arrive on time within a specified synchronization cycle and results in the failure of accurate time synchronization of the adjacent vehicles. To reduce the error caused by clock state immeasurability due to packet loss, an observer was introduced to accurately estimate the immeasurable clock state. The specific observation equation of the observer is as follows:

$$\widehat{\boldsymbol{x}}_i(k+1) = \boldsymbol{A}\widehat{\boldsymbol{x}}_i(k) + \boldsymbol{B}\boldsymbol{u}_i(k) + \boldsymbol{L}(y_i(k) - \widehat{y}_i(k)) \tag{12}$$

where $\widehat{\boldsymbol{x}}_i(k+1)$ and $\widehat{\boldsymbol{x}}_i(k)$ are the clock state estimates of the adjacent vehicles at time $k+1$ and time k, respectively; $\widehat{y}_i(k)$ is the clock state output estimate of the adjacent vehicles at time k.

In order to solve the observer gain matrix $\boldsymbol{L}$, the error vector $\boldsymbol{e}$ of the actual state and the observer state estimate was introduced, and the formula is as follows:

$$\boldsymbol{e}_i(k) = \boldsymbol{x}_i(k) - \widehat{\boldsymbol{x}}_i(k) \tag{13}$$

With Equations (10) and (12) put in, Equation (13) is expanded and simplified as

$$\boldsymbol{e}_i(k+1) = (\boldsymbol{A} - \boldsymbol{LC})\boldsymbol{e}_i(k) \tag{14}$$

Since $\boldsymbol{A}$ and $\boldsymbol{C}$ are constants defined by the system, $\boldsymbol{L}$ is generally calculated by pole placement with all eigenvalues for the matrix $\boldsymbol{A}$-$\boldsymbol{LC}$ within the unit circle.

It can be seen from Equation (14) that the poles of matrix $\boldsymbol{A}$-$\boldsymbol{LC}$ determine whether the estimation error $\boldsymbol{e}$ of the observer can finally converge to 0. After obtaining the state estimate from the observer in the case of packet loss, a random variable $\gamma[k]$ following the Bernoulli distribution was introduced to describe the PTP message loss of the k-th synchronization cycle to further describe the phenomenon of packet loss due to the 5G-R wireless channel. If $\gamma[k]$ takes the value 1 with probability $1-p$, indicating that no message loss occurs in the cycle, then the clock state at the current time can be measured and calculated by Equation (10). If $\gamma[k]$ takes the value 0 with probability p, indicating that a message loss occurs and the clock state cannot be measured in the k-th cycle, then the clock state estimate obtained by Equation (12) can be used to replace the immeasurable null state value for calculation.

Combining Equations (10)–(12) and considering packet loss, the state space model of the adjacent vehicles was finally established as

$$\begin{cases} \boldsymbol{x}_i(k+1) = \boldsymbol{A}\boldsymbol{x}_i(k) + \boldsymbol{B}\boldsymbol{u}_i(k) + \boldsymbol{\omega}_i(k) & \gamma[k] = 1 \\ \widehat{\boldsymbol{x}}_i(k+1) = \boldsymbol{A}\widehat{\boldsymbol{x}}_i(k) + \boldsymbol{B}\boldsymbol{u}_i(k) + \boldsymbol{L}(y_i - \widehat{y}_i) & \gamma[k] = 0 \\ y_i(k) = \begin{cases} \boldsymbol{C}\boldsymbol{x}_i(k) + \nu_i(k) & \gamma(k) = 1 \\ \boldsymbol{C}\widehat{\boldsymbol{x}}_i(k) + \nu_i(k) & \gamma(k) = 0 \end{cases} \end{cases} \tag{15}$$

4.2 Predictive model

After the state space model for V2V communication was established, the clock state predictive model for V2V communication was established. An incremental state space predictive model was used instead of traditional predictive models to eliminate the influence of the clock's uncertain input disturbance caused by the external environment and its uncertain output disturbance caused by the 5G-R wireless channel on the predictive output results.

Let the short duration disturbance of the 5G-R wireless channel remain unchanged, and rewrite Equation (15) into an incremental form as

$$\begin{cases} \Delta\boldsymbol{x}_i(k+1) = \begin{cases} \boldsymbol{A}\Delta\boldsymbol{x}_i(k) + \boldsymbol{B}\Delta\boldsymbol{u}_i(k) & \gamma(k) = 1 \\ \boldsymbol{A}\Delta\widehat{\boldsymbol{x}}_i(k) + \boldsymbol{B}\Delta\boldsymbol{u}_i(k) & \gamma(k) = 0 \end{cases} \\ \Delta y_i(k) = \boldsymbol{C}\Delta\boldsymbol{x}_i(k) \end{cases} \tag{16}$$

Based on the incremental state Equation (16), an additional state variable output y was introduced to expand the original model, obtaining the incremental state vector as

$$\overline{\boldsymbol{x}}_i(k) = \begin{pmatrix} \Delta\boldsymbol{x}_i(k) \\ y_i(k) \end{pmatrix} \tag{17}$$

Equations (10), (16) and (17) were combined to obtain an extended model with incremental output, that is the predictive model, as below

$$\begin{cases} \overline{\boldsymbol{x}}_i(k+1) = \breve{\boldsymbol{A}}\overline{\boldsymbol{x}}_i(k) + \breve{\boldsymbol{B}}\Delta\boldsymbol{u}_i(k) \\ \overline{y}_i(k) = \breve{\boldsymbol{C}}\overline{\boldsymbol{x}}_i(k) \end{cases} \tag{18}$$

with

$$\breve{\boldsymbol{A}} = \begin{pmatrix} \boldsymbol{A} & 0 \\ \boldsymbol{CA} & \boldsymbol{I} \end{pmatrix}$$

$$\breve{\boldsymbol{B}} = \begin{pmatrix} \boldsymbol{B} \\ \boldsymbol{CB} \end{pmatrix}$$

$$\breve{\boldsymbol{C}} = (\boldsymbol{0} \quad \boldsymbol{I})$$

where $\breve{\boldsymbol{A}}$ is the transition matrix from the current state $\overline{\boldsymbol{x}}_i(k)$ to the next state $\overline{\boldsymbol{x}}_i(k+1)$; $\breve{\boldsymbol{B}}$ is the transition matrix from the control input increment $\Delta\boldsymbol{u}_i(k)$ to the next state $\overline{\boldsymbol{x}}_i(k+1)$; $\breve{\boldsymbol{C}}$ is the transition matrix from the current state to output $\overline{y}_i(k)$.

4.3 Multistep prediction

After the predictive model was established, the goal of time synchronization for V2V communication can be achieved with phase and frequency offsets at the clock node i of the adjacent vehicles taken as the states of the closed-loop system and through time synchronization of the adjacent vehicles with the reference clock by adjusting the control input $\boldsymbol{u}_i$ of the closed-loop system. Assuming that the prediction step size of the clock node state is Np and the control step size of the control quantities in the prediction horizon is Nc, then the predicted state value of each clock node of the adjacent vehicles will be obtained with Nc control quantities used in the future Np time synchronization cycles

$$\begin{aligned} \overline{\boldsymbol{x}}_i(k+N\mathrm{p}|k) &= \breve{\boldsymbol{A}}^{N\mathrm{p}}\overline{\boldsymbol{x}}_i(k) + \breve{\boldsymbol{A}}^{N\mathrm{p}-1}\breve{\boldsymbol{B}}\Delta\boldsymbol{u}_i(k) + \breve{\boldsymbol{A}}^{N\mathrm{p}-2}\breve{\boldsymbol{B}}\Delta\boldsymbol{u}_i(k+1|k) + \cdots \\ &+ \breve{\boldsymbol{A}}^{N\mathrm{p}-N\mathrm{c}}\breve{\boldsymbol{B}}\Delta\boldsymbol{u}_i(k+N\mathrm{c}-1|k) \end{aligned} \tag{19}$$

where $k+1|k$ is the predicted state value of the $k+1$-th synchronization cycle at the k-th synchronization cycle.

Similarly, the predicted output value of each clock node of the adjacent vehicles within Np cycles from the k-th cycle can be obtained as

$$\begin{aligned} \overline{y}_i(k+N\mathrm{p}|k) &= \breve{\boldsymbol{C}}\breve{\boldsymbol{A}}^{N\mathrm{p}}\overline{\boldsymbol{x}}_i(k) + \breve{\boldsymbol{C}}\breve{\boldsymbol{A}}^{N\mathrm{p}-1}\breve{\boldsymbol{B}}\Delta\boldsymbol{u}_i(k) + \breve{\boldsymbol{C}}\breve{\boldsymbol{A}}^{N\mathrm{p}-2}\breve{\boldsymbol{B}}\Delta\boldsymbol{u}_i(k+1|k) + \cdots \\ &+ \breve{\boldsymbol{C}}\breve{\boldsymbol{A}}^{N\mathrm{p}-N\mathrm{c}}\breve{\boldsymbol{B}}\Delta\boldsymbol{u}_i(k+N\mathrm{c}-1|k) \end{aligned} \tag{20}$$

Equation (20) is further integrated into a matrix form and is obtained as

$$\boldsymbol{Y}_i(k) = \boldsymbol{F}\overline{\boldsymbol{x}}_i(k) + \boldsymbol{\Phi}\Delta\boldsymbol{U}_i(k) \tag{21}$$

with

$$\boldsymbol{Y}_i(k) = \begin{pmatrix} \overline{y}_i(k+1|k) \\ \overline{y}_i(k+2|k) \\ \vdots \\ \overline{y}_i(k+N\mathrm{c}|k) \\ \vdots \\ \overline{y}_i(k+N\mathrm{p}|k) \end{pmatrix}$$

$$\boldsymbol{F} = \begin{pmatrix} \breve{\breve{\boldsymbol{C}}}\breve{\boldsymbol{A}} \\ \breve{\boldsymbol{C}}\breve{\boldsymbol{A}}^2 \\ \vdots \\ \breve{\boldsymbol{C}}\breve{\boldsymbol{A}}^{N\mathrm{c}} \\ \vdots \\ \breve{\boldsymbol{C}}\breve{\boldsymbol{A}}^{N\mathrm{p}} \end{pmatrix}$$

$$\boldsymbol{\Phi} = \begin{pmatrix} \breve{\breve{\boldsymbol{C}}}\breve{\boldsymbol{B}} & 0 & \cdots & 0 \\ \breve{\boldsymbol{C}}\breve{\boldsymbol{A}}\breve{\boldsymbol{B}} & \breve{\breve{\boldsymbol{C}}}\breve{\boldsymbol{B}} & \cdots & 0 \\ \breve{\boldsymbol{C}}\breve{\boldsymbol{A}}^2\breve{\boldsymbol{B}} & \breve{\boldsymbol{C}}\breve{\boldsymbol{A}}\breve{\boldsymbol{B}} & \cdots & 0 \\ \vdots & \vdots & \vdots & \vdots \\ \breve{\boldsymbol{C}}\breve{\boldsymbol{A}}^{N\mathrm{c}}\breve{\boldsymbol{B}} & \breve{\boldsymbol{C}}\breve{\boldsymbol{A}}^{N\mathrm{c}-1}\breve{\boldsymbol{B}} & \cdots & \breve{\breve{\boldsymbol{C}}}\breve{\boldsymbol{A}}\breve{\boldsymbol{B}} \\ \vdots & \vdots & \vdots & \vdots \\ \breve{\boldsymbol{C}}\breve{\boldsymbol{A}}^{N\mathrm{p}-1}\breve{\boldsymbol{B}} & \breve{\boldsymbol{C}}\breve{\boldsymbol{A}}^{N\mathrm{p}-2}\breve{\boldsymbol{B}} & \cdots & \breve{\boldsymbol{C}}\breve{\boldsymbol{A}}^{N\mathrm{p}-N\mathrm{c}}\breve{\boldsymbol{B}} \end{pmatrix}$$

$$\Delta \boldsymbol{U}_i(k) = \begin{pmatrix} \Delta \boldsymbol{u}_i(k) \\ \Delta \boldsymbol{u}_i(k+1|k) \\ \vdots \\ \Delta \boldsymbol{u}_i(k+N\mathrm{c}-1|k) \end{pmatrix}$$

where $\boldsymbol{Y}_i(k)$ is the predicted output matrix within Np steps from time k+1; $\Delta \boldsymbol{U}_i(k)$ is the control input increment matrix within Nc steps from time k; $\boldsymbol{F}$ and $\boldsymbol{\Phi}$ are the coefficient matrixes of clock states of adjacent vehicles and control input increment $\Delta \boldsymbol{U}_i$, respectively.

4.4 Rolling optimization and feedback correction

After obtaining the predicted output values of the clock states of the adjacent vehicles in the next Np cycles, it is necessary to continuously adjust and use the control input increment $\Delta \boldsymbol{u}$ to correct the clock state so that the predicted output gradually converges to the reference time r, thus synchronizing the local clocks of the adjacent vehicles with the reference clock.

The optimal control input increment $\Delta \boldsymbol{u}$ can be solved by minimizing the cost function $\boldsymbol{J}$ of the MPC. Generally, the quadratic matrix of error and output increment is used as the cost function. If the reference time provided by gNB is $\boldsymbol{R}$, the cost function $\boldsymbol{J}$ is defined as

$$\boldsymbol{J} = (\boldsymbol{R} - \boldsymbol{Y}_i(k))^{\mathrm{T}}(\boldsymbol{R} - \boldsymbol{Y}_i(k)) + \Delta \boldsymbol{u}_i{}^{\mathrm{T}}(k)\boldsymbol{Q}\Delta \boldsymbol{u}_i(k) \tag{22}$$

where the first term on the right side is expressed as the error between the reference input $\boldsymbol{R}$ and the output of the predictive model, and its value reflects the synchronization performance

of the adjacent vehicles during V2V communication; the second item reflects the stability of time synchronization in V2V communication, in which $\boldsymbol{Q}$ is a diagonal matrix that restricts control input increment $\Delta \boldsymbol{u}$ to avoid poor stability due to excessive increment values.

Substituting Equation (21) into Equation (22), the cost function $\boldsymbol{J}$ will be further rewritten as

$$\boldsymbol{J} = (\boldsymbol{R} - \boldsymbol{F}\boldsymbol{x}_i(k))^{\mathrm{T}}(\boldsymbol{R} - \boldsymbol{F}\boldsymbol{x}_i(k)) - 2\Delta \boldsymbol{u}_i{}^{\mathrm{T}}(k)\boldsymbol{\Phi}^{\mathrm{T}}(\boldsymbol{R} - \boldsymbol{F}\boldsymbol{x}_i(k)) + \Delta \boldsymbol{u}_i{}^{\mathrm{T}}(k)(\boldsymbol{\Phi}^{\mathrm{T}}\boldsymbol{\Phi} + \boldsymbol{Q})\Delta \boldsymbol{u}_i(k) \tag{23}$$

To obtain the optimal control input increment $\Delta \boldsymbol{u}$, the first-order partial derivative of $\Delta \boldsymbol{u}$ in Equation (23) is solved and obtained as

$$\frac{\partial \boldsymbol{J}}{\partial \Delta \boldsymbol{u}_i(k)} = -2\boldsymbol{\Phi}^{\mathrm{T}}(\boldsymbol{R} - \boldsymbol{F}\boldsymbol{x}_i(k)) + 2(\boldsymbol{\Phi}^{\mathrm{T}}\boldsymbol{\Phi} + \boldsymbol{Q})\Delta \boldsymbol{u}_i(k) \tag{24}$$

Let the first-order partial derivative of $\boldsymbol{J}$ be 0, and the optimal solution of $\Delta \boldsymbol{u}_i(k)$ of clocks of the adjacent vehicles in the k-th synchronization cycle can be obtained as

$$\Delta \boldsymbol{u}_i(k) = (\boldsymbol{\Phi}^{\mathrm{T}}\boldsymbol{\Phi} + \boldsymbol{Q})\boldsymbol{\Phi}^{\mathrm{T}}(\boldsymbol{R} - \boldsymbol{F}\boldsymbol{x}_i(k)) \tag{25}$$

During time synchronization for V2V communication under 5G-R, due to the end-to-end delay (Yu, 2021), in order that the model is more in line with the actual situation, it is necessary to further constrain the value of the clock phase optimal control input increment $\Delta u_{i\theta}$ in Equation (25) as

$$|\Delta u_{i\theta}(k)| \leq \Delta u_{\max} \tag{26}$$

where $\Delta u_{\max}$ takes the upper limit 150 ms of end-to-end delay (Yu, 2021).

Finally, the optimal control input $\boldsymbol{u}_i(k)$ of the whole-time synchronization process for V2V communication in the k-th synchronization cycle is obtained as

$$\boldsymbol{u}_i(k) = \boldsymbol{u}_i(k-1) + \Delta \boldsymbol{u}_i(k) \tag{27}$$

where $\Delta \boldsymbol{u}_i(k)$ is the optimal control input increment.

After obtaining the optimal control input $\boldsymbol{u}$ of the k-th synchronization cycle, it can be used as a feedback input to time synchronization in V2V communication to perform feedback correction of the cycle. The above steps were iterated continuously so that the clocks of adjacent vehicles can keep track of the reference clock and realize time synchronization in different scenarios of V2V communication under 5G-R.

5. Analysis of simulation results

In order to verify the effectiveness of the proposed method in V2V communication under 5G-R, MATLAB software was used to simulate the synchronization process in the scenarios with and without a repeater, respectively.

5.1 Simulation analysis of synchronization in V2V communication with a repeater

5.1.1 Simulation of synchronization process. First, it was simulated in the scenario of time synchronization process in V2V communication with a repeater. According to the requirements of the 3rd Generation Partnership Project (3GPP), the initial clock frequency offset α_{0i} of the adjacent vehicles was set as 0.05 ppm (Teng, 2021). Additionally, let the input

and output disturbance variances be σ_θ^2, σ_α^2 and σ_{iM}^2 be 5×10^{-11}, 5×10^{-8} and 10^{-6} (Chen, 2020), and the packet loss probability p be 10^{-3} according to the Quality of Service (QoS) indicator. Assuming the expected pole of the closed loop $\boldsymbol{P}$=(0.1 0.2), the observer gain matrix $\boldsymbol{L}$=(1.7 1.44)$^{\mathrm{T}}$ can be calculated according to the pole placement method. Assuming the number of simulated synchronization cycles is 60 and the local time of adjacent vehicles and their corresponding repeater station gNB is 0.4, 0.2 and 1 ms, respectively, the MPC-based time synchronization process of V2V communication under 5G-R with a repeater was obtained, as shown in Figure 5.

As can be seen from Figure 5, as synchronization cycles increase, the time of gNB, the reference clock for the time synchronization process in the scenario with a repeater, remains unchanged, while clocks of the adjacent vehicles with different initial times can dynamically adjust their own time and gradually align to the gNB reference time in a limited time with the increase of synchronization cycles, realizing the consistency with the gNB reference clock and completing the time synchronization process for V2V communication. The simulation results in Figure 5 show that time synchronization for V2V communication under 5G-R with a repeater can be completed by using the method in this paper.

5.1.2 Comparison of synchronization performance. In order to verify the effectiveness of this method in the scenario of V2V communication with a repeater, this method was compared with the time synchronization method based on PID controllers (Wang, Qi *et al.*, 2020) and the MPC method based on error increment (Zhang *et al.*, 2022) in terms of convergence time, clock offset and system stability.

First, comparison of convergence time, as the number of cycles required for the maximum logical clock error $e \to 0$ in the whole synchronization process, is an important index for evaluating clock synchronization methods. For ease of comparing different methods' capability to track the reference time, the initial time of trains was uniformly set to 0 ms for the methods by Wang, Qi *et al.* (2020), Zhang *et al.* (2022) and this paper, and the reference clock time of repeater station gNB in the whole synchronization process was set to 1 ms. The convergence of the three methods used in the scenario of V2V communication with a repeater was obtained, as shown in Figure 6.

As can be seen, the methods require different numbers of synchronization cycles to realize time synchronization between adjacent vehicles; time synchronization between the adjacent vehicles and the gNB cannot be realized until about the 40th synchronization cycle with the PID-based synchronization method (Wang, Qi *et al.*, 2020) and the method based on error

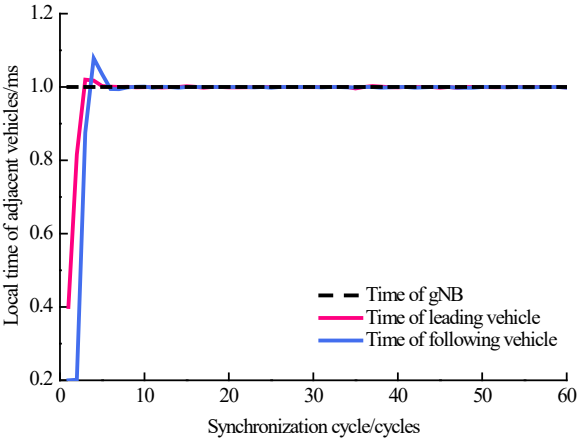

Figure 5.
MPC-based time synchronization for V2V communication with a repeater

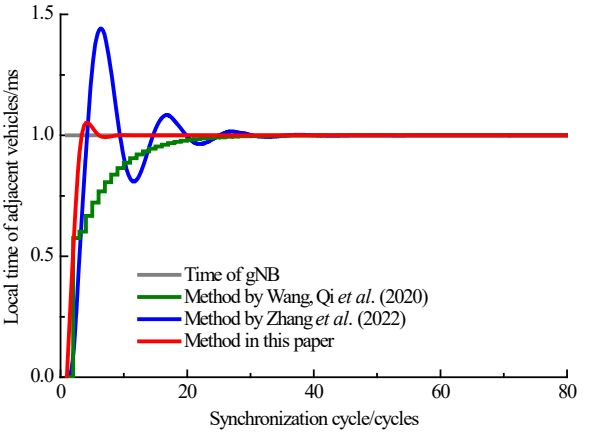

Figure 6.
Comparison of convergence with a repeater

increment MPC (Zhang *et al.*, 2022); while convergence with the method in this paper is achieved after 8 synchronization cycles, about one-fifth that of the former two methods. This is because the PID control method adopted by Wang, Qi *et al.* (2020) has poor adaptability to fast time variation and is prone to frequent modification of control parameters and long duration (Liu, Wang, & Zhao, 2022), resulting in slow convergence, and the error-based MPC synchronization method adopted by Zhang *et al.* (2022) takes the clock error as the model increment during time synchronization, in which case its control quantities will fluctuate rapidly when the clock error fluctuates rapidly due to time variation of 5G-R wireless channel and packet loss, also resulting in slow convergence. Conversely, with the method in this paper, the synchronization process of V2V communication can be completed more quickly than the methods by Wang, Qi *et al.* (2020) and Zhang *et al.* (2022), resulting in a faster convergence speed, thanks to the comprehensive consideration of the impact of packet loss and 5G-R channel time variation on the synchronization process.

Second, clock offset was compared, when the mean and standard deviation were introduced for quantitative comparison, and the standard deviation σ was calculated using the equation below:

$$\sigma = \sqrt{\frac{1}{N}\sum_{i=1}^{N}(z_i - \bar{z})^2} \tag{28}$$

where z_i is the input value; $\bar{z}$ is the mean of the input value; N is the number of samples.

Table 1 gives the mean of clock offset obtained by the three methods and the standard deviation of clock offset calculated by Equation (28).

As shown, both the mean and standard deviation values obtained by the methods by Wang, Qi *et al.* (2020) and Zhang *et al.* (2022) are greater than those by the method in this

Table 1.
Clock offset results by different methods

Method	Mean deviation/ms	Standard deviation/ms
Method by Wang, Qi *et al.* (2020)	0.0384	0.1266
Method by Zhang *et al.* (2022)	0.0151	0.1715
Method in this paper	0.0148	0.1104

paper. Therefore, the method in this paper has smaller errors and higher precision in synchronization compared with the other two methods because the smaller the standard deviation, an index reflecting the dispersion of samples, the smaller the clock synchronization error, and the closer to the standard reference value.

Finally, the system stability was compared. The variation of system control input increment $\Delta u_{i\theta}$ reflects the system stability, and Figure 7 shows the variation with different methods in the scenario with a repeater.

It can be seen from Figure 7 that the control input increment $\Delta u_{i\theta}$ of MPC controllers in the method of this paper tends to stabilize rapidly when the number of synchronization cycles increases, while the control input increment $\Delta u_{i\theta}$ of the methods by Wang, Qi *et al.* (2020) and Zhang *et al.* (2022) fluctuates violently since these methods do not consider the influence of clock error caused by packet loss in the synchronization process; the method in this paper can effectively ensure the stability of the time synchronization process of V2V communication with a repeater.

It can be comprehensively concluded that, in the cases of V2V communication under 5G-R with a repeater, the proposed method can complete time synchronization of V2V communication more effectively through the above analysis of convergence time, clock offset and system stability.

5.2 Simulation analysis of synchronization in V2V communication without a repeater

5.2.1 Simulation of synchronization process. After completing the analysis of synchronization in V2V communication with a repeater, the time synchronization process in the scenario without a repeater was simulated and analyzed. In the scenario without a repeater, it is necessary to set up a virtual reference clock as the master clock for synchronization between the adjacent vehicles as there is no gNB repeater station to provide a standard reference clock, and the vehicles achieve time synchronization by tracking the time of the virtual reference clock.

Assuming there are 10 simulated synchronization cycles, the initial times of the adjacent vehicles remain 0.4 and 0.2 ms, respectively, and the dynamic coefficient β is 0.4. Then the synchronization process in repeater-free V2V communication was simulated using the method in this paper, as shown in Figure 8.

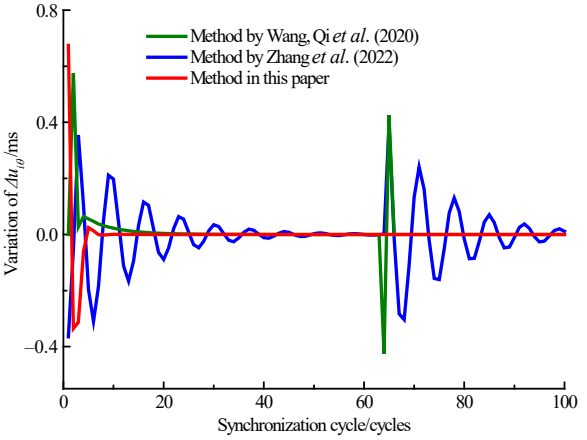

Figure 7.
Comparison of system stability with a repeater

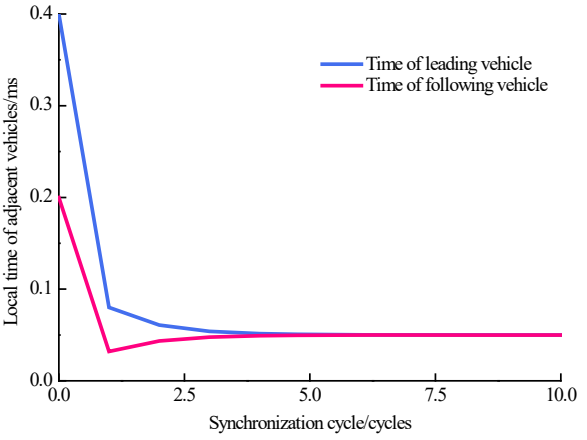

Figure 8.
Time synchronization process of repeater-free V2V communication

It can be seen from Figure 8 that, as synchronization cycles gradually increase, the adjacent vehicles can dynamically adjust their own clock states and synchronize their clocks with different initial times in a limited time through the exchange of time information even when there is no physical reference clock, thus realizing time synchronization of direct V2V communication without a repeater.

5.2.2 Comparison of synchronization performance. In order to verify the effectiveness of this method in time synchronization process of repeater-free V2V communication, its performance was analyzed from two aspects of convergence time and clock offset, and compared with that of the synchronization method in repeater-free scenario proposed by Phan and Kim (2021). For easier comparative analysis, it was assumed that the initial time of the leading vehicle was 0.4 ms and the initial time of the following vehicle was 0.2 ms for both methods by Phan and Kim (2021) and in this paper.

First, the convergence time in the repeater-free scenario of V2V communication was compared between different methods, and the comparison results were obtained through simulation, as shown in Figure 9.

It can be seen from Figure 9 that the time synchronization method adopted by Phan and Kim (2021) is based on average consensus and realizes time synchronization between vehicles

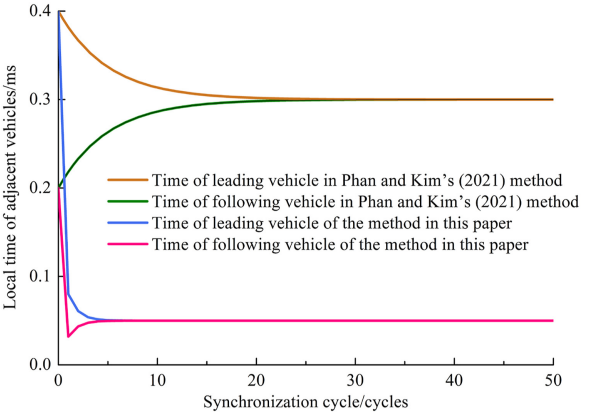

Figure 9.
Comparison results of convergence time in the scenario without a repeater

within 30 synchronization cycles, while the MPC-based synchronization method proposed in this paper realizes time synchronization between adjacent vehicles within only 5 synchronization cycles, greatly shortening the convergence time; the primary cause for this large difference in convergence time is that Phan and Kim (2021) use the consensus theory as their synchronization method, and as a distributed cooperation method, this method realizes global consensus mainly with the help of the value of the input control quantity, which is mainly calculated according to the local information of adjacent nodes (Zhang, Xue, & Gao, 2020) and largely influenced by the uncertain output disturbance brought about by the 5G-R wireless channel, resulting in long convergence time; with the method in this paper, however, adjacent trains dynamically adjust their own clocks through the exchange of time information, and the synchronization cooperativity and convergence speed are thus improved.

Finally, the clock offset between the adjacent vehicles in repeater-free V2V communication was compared, and the comparison results were obtained through simulation, as shown in Figure 10.

It can be seen from Figure 10 that in the repeater-free mode, the clock offset of the adjacent vehicles can be gradually reduced and converged as synchronization cycles increase with both methods; Phan and Kim's (2021) method fails to realize time synchronization in the real sense, and there is still a certain clock offset between the adjacent vehicles; on the other hand, the clock offset between the adjacent vehicles is 0 with the method in this paper, indicating that this method has higher synchronization precision, better realizes high-precision time synchronization between vehicles without a repeater under 5G-R and can meet the time synchronization precision requirements of V2V communication under 5G-R (Teng, 2021).

According to the above convergence time and clock offset analysis, it can be concluded that the proposed method has a faster convergence speed and higher synchronization precision than the compared methods and can better realize time synchronization in scenarios of repeater-free V2V communication under 5G-R.

5.3 Influence of different delays and jitter levels on synchronization

The influence of 5G-R delay and jitter on the time synchronization process was further analyzed in this paper. First, the influence of 5G-R delay was analyzed. To compare the influence of different delays on the synchronization process, the delays of 19, 56 and 100 ms were taken according to the packet delay range under 5G-R (Zhou, 2021), and the change of

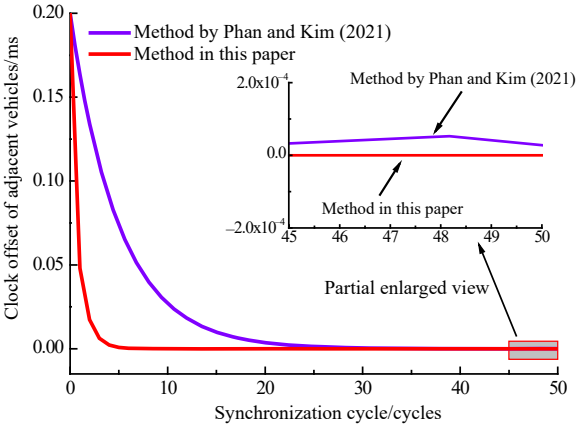

Figure 10.
Comparison of clock offset of adjacent vehicles in repeater-free scenario

control input increment $\Delta u_{i\theta}$ of the method in this paper with the synchronization cycle was clarified through simulation, as shown in Figure 11.

It can be seen from Figure 11 that the larger the 5G-R delay, the greater the change of the control input increment $\Delta u_{i\theta}$. Since the control input increment represents system stability, it indicates that the delay can affect the stability of the time synchronization process under 5G-R, and that the larger the delay, the more unstable the synchronization process. As the number of synchronization cycles increases, the value of control input increment $\Delta u_{i\theta}$ gradually becomes stable, which indicates that the method in this paper can effectively eliminate the influence of time delay on synchronization, and further verifies its effectiveness.

Then, the influence of 5G-R transmission jitter on synchronization was analyzed. Jitter occurs when PTP synchronization messages are transmitted on time-varying channels of high-speed railways, resulting in asymmetric transmission of PTP protocol links. Assuming that the initial train clock is 20 ms, the reference clock is 50 ms and the transmission jitter is random noise, then the influence of different jitter levels, represented by different values of noise variance $\sigma^2_{i\mathrm{M}}$, on the synchronization process was obtained and shown in Figure 12.

It can be seen from Figure 12 that the greater the noise variance $\sigma^2_{i\mathrm{M}}$, that is the greater the 5G-R jitter, the more violently the train time will fluctuate in the synchronization process.

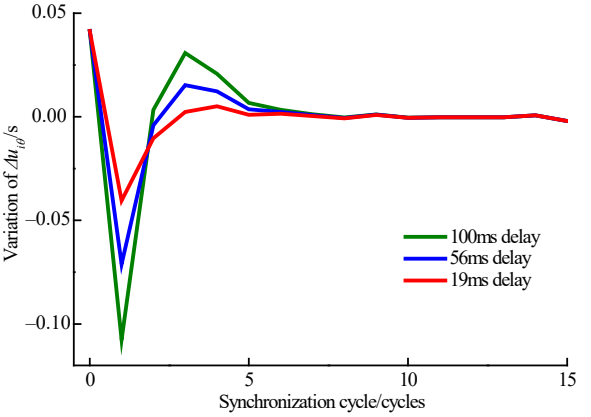

Figure 11.
Influence of different delays on synchronization

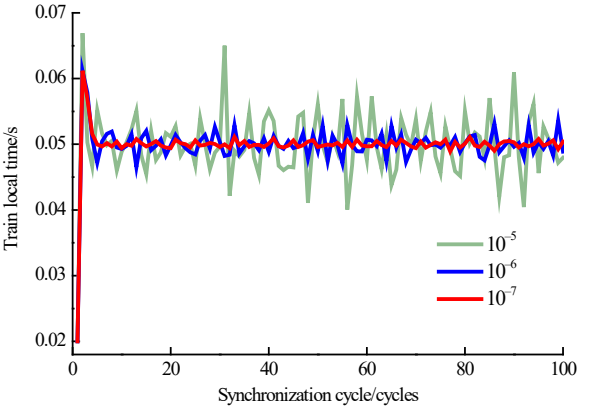

Figure 12.
Influence of different jitter levels on synchronization

This is because in the 5G-R scenario, the jitter level determines the degree of interference to the transmission of PTP synchronization messages. The greater the jitter level, the greater the influence on time synchronization.

6. Conclusions

(1) This paper proposed an MPC-based time synchronization method for V2V communication under 5G-R. Through the construction of MPC controllers for clocks of adjacent vehicles, time synchronization was realized for V2V communication under 5G-R by using control means such as multistep prediction, rolling optimization, and feedback correction.

(2) In view of the problems of low synchronization precision and slow convergence speed caused by packet loss with existing synchronization methods, the observer equation was introduced to estimate the clock state of the adjacent vehicles in case of packet loss, which reduces the impact of clock error caused by packet loss on the synchronization process and improves the synchronization precision of V2V communication.

(3) The simulation test results with and without repeaters indicate that the proposed method can achieve time synchronization of V2V communication in two situations.

(4) Compared with other methods, the method in this paper provides a faster convergence speed and higher synchronization precision regardless of whether there is a repeater or not. The research results of this paper provide some theoretical references for V2V synchronous wireless communication under 5G-R technology.

References

Alfaro, C., Guzman, R., De Vicuña, L. G., Miret, J., & Castilla, M. (2022). Dual-loop continuous control set model-predictive control for a three-phase unity power factor rectifier. *IEEE Transactions on Power Electronics*, *37*(2), 1447–1460.

Chen, S. (2020). *Research on fast time-varying characteristics of high speed rail wireless channel and key technology of channel equalization* MA thesis. Beijing Jiaotong University, Beijing (in Chinese).

Ding, Y. (2020). Study on soft handover technology in high speed train-wayside broadband communication system. *Journal of the China Railway Society*, *42*(7), 87–94 (in Chinese).

Dou, Y., Li, Y., Li, H., Bao, J., & Lin, W. (2021). Isolation between vehicle-mounted antennas for 350 $km \cdot h^{-1}$ Chinese standard EMU and minimum spacing. *China Railway Science*, *42*(1), 130–136 (in Chinese).

Fan, D., Liu, Y., Li, X., & Chen, R. (2021). Research of high performance time keeping method based on crystal oscillator. *Journal of Time and Frequency*, *44*(1), 26–32 (in Chinese).

Jia, P. Y., Wang, X. B., & Zheng, K. (2020). Distributed clock synchronization based on intelligent clustering in local area industrial IoT systems. *IEEE Transactions on Industrial Informatics*, *16*(6), 3697–3707.

Koo, Y. C., & Mahyuddin, M. N. (2019). Time synchronization in WSAN using sliding mode and PID control. *10th International Conference on Robotics, Vision, Signal Processing and Power Applications* (pp. 435–441) Singapore: Springer.

Lai, W. L., Shieh, C. S., Chou, F. S., & Hsu, C. Y. (2020). Handover management for D2D communication in 5G networks. *2020 2nd International Conference on Computer Communication and the Internet (ICCCI)* (pp. 64–69) New York: IEEE Press.

Liu, Q., Wang, Z., & Zhao, L. (2022). Vehicle tracking optimization based on adaptive LOS guidance and MPC control. *Journal of Harbin Institute of Technology*, *54*(1), 96–104 (in Chinese).

Novaes, C., Freire, I., Klautau, A., & Almeida, I. (2021). Analysis of Kalman filtering for clock synchronization in PTP-unaware networks. *2021 IEEE Latin-American Conference on Communications* (pp. 1–6) New York: IEEE Press.

Phan, L. A., & Kim, T. (2021). Fast consensus-based time synchronization protocol using virtual topology for wireless sensor networks. *IEEE Internet of Things Journal*, *8*(9), 7485–7496.

Schennato, L., & Fiorentin, F. (2011). Average TimeSynch: A consensus-based protocol for clock synchronization in wireless sensor networks. *Automatica*, *47*(9), 1878–1886.

Seijo, Ó., López-fernández, J. A., Bernhard, H. P., & Val, I. (2020). Enhanced timestamping method for subnanosecond time synchronization in IEEE 802.11 over WLAN standard conditions. *IEEE Transactions on Industrial Informatics*, *16*(9), 5792–5805.

Shi, F. R., Tuo, X. G., Ran, L. L., Ren, Z. W., & Yang, S. X. (2020). Fast convergence time synchronization in wireless sensor networks based on average consensus. *IEEE Transactions on Industrial Informatics*, *16*(2), 1120–1129.

Shi, F. R., Tuo, X. G., Yang, S. X., Lu, J., & Li, H. L. (2020). Rapid-flooding time synchronization for large-scale wireless sensor networks. *IEEE Transactions on Industrial Informatics*, *16*(3), 1581–1590.

Shivaaraman, N., Schuster, P., Ramanathan, S., Easwaran, A., & Steinhorst, S. (2021). Cluster-based network time synchronization for resilience with energy efficiency. *2021 IEEE Real-Time Systems Symposium* (pp. 149–161). New York: IEEE Press.

Son, K. J., & Chang, T. G. (2020). Distributed nodes-based collaborative sustaining of precision clock synchronization upon master clock failure in IEEE 1588 system. *Sensors*, *20*(20), 5784.

Teng, L. (2021). Support for 5G-R with time synchronization architecture for railway. *Railway Signalling & Communication*, *57*(9), 48–51, 57 (in Chinese).

Wang, T. (2020). Key railway 5G technology analysis and development route. *China Railway*, *11*, 1–9 (in Chinese).

Wang, H., Chen, L. Q., Gong, P. F., & Li, M. (2020). Skew estimation based on weighted median for average consensus time synchronization in the presence of communication delay. *IEEE Wireless Communications Letters*, *9*(9), 1384–1388.

Wang, K., Qi, X. P., & Li, P. W. (2020). Design of high precision synchronous data acquisition system with temperature compensation. *2020 IEEE International Conference on Artificial Intelligence and Information Systems* (pp. 235–238) New York: IEEE Pres.

Wang, P., Li, K., & Liu, Y. (2016). Application research of train control system based on train to train communication. *Railway Signalling and Communication*, *52*(7), 62–65, 70 (in Chinese).

Yu, Y. (2021). *Research on key technologies of train-ground communication for CTCS-3 train control service based on 5G-R*. Beijing: Beijing Jiaotong University (in Chinese).

Zhang, P., Xue, H., & Gao, S. (2020). Distributed adaptive fault-tolerance consensus control for multi-agent system. *Acta Aeronautica et Astronautica Sinica*, *41*(3), 323539 (in Chinese).

Zhang, W., Wu, W., Teng, Y., Gong, P., & Tang, Y. (2022). Moving-base unmanned underwater vehicles docking control based on satisfactory model predictive control with constrained conditions. *Journal of Harbin Engineering University*, *2022*(1), 1–12 (in Chinese).

Zhou, H. (2021). *Research on network inspection system of 5G-R* MA thesis. China Academy of Railway Sciences, Beijing (in Chinese).

Corresponding author
Yong Chen can be contacted at: edukeylab@126.com